SAND2017-13836C

Maximizing The Revenue of Energy Storage Systems in Market Areas Considering Nonlinear Storage Efficiencies

Tu A. Nguyen, *Member, IEEE,* Raymond H. Byrne, *Fellow, IEEE,* Babu R. Chalamala, *Fellow, IEEE,* and Imre Gyuk

***Abstract*—Techno-economic analyses of energy storage currently use constant-efficiency energy flow models. In practice, charge/discharge efficiency of energy storage varies as a function of state-of-charge, temperature, charge/discharge power. Therefore, using the constant-efficiency energy flow models will cause suboptimal results. This work focuses on incorporating nonlinear energy flow models based on nonlinear efficiency models in the revenue maximization problem of energy storage. Dynamic programming is used to solve the optimization problem. A case studies is conducted to maximize the revenue of a Vanadium Redox Flow Battery (VRFB) system in PJM's energy and frequency regulation market.**

***Index Terms*—Energy storage, vanadium redox battery, li-ion battery, energy arbitrage, frequency regulation, dynamic programming, non-linear battery model.**

I. Introduction

In the last decade, grid modernization has become an imperative task due to the aging grid infrastructure, the rapid growth of renewable energy and the changes in energy policies. New technologies and development trends have emerged to transform today's grid toward a smarter, more reliable and more distributed grid in the future [1]. Among the latest development trends, the grid integration of energy storage systems (ESS) has shown its great potential to provide multiple benefits to the grid as well as to the customers. On the grid's side, energy storage can help grid operators better manage the variability of the generation and demand by providing ancillary services such as frequency regulation and spinning/non-spinning reserve [2]. On the customers' side, energy storage can also provide a wide range of applications such as on-site back-up power, PV utilization, demand charge reduction or time-of-use management [3].

In order to realize the potential of ESSs for the grid-side and customer-side services, it is crucial to assess the overall economic gains of energy storage deployments considering their technical benefits to the grid as well as their limits in energy efficiency [4]. In the literature, a number of works have evaluated the benefits of ESSs for different applications. In [5], a mathematical framework of planning and control is proposed to maximize the profit of battery energy storage systems (BESS) for primary frequency control. In [6–9], potential revenues of ESSs for energy arbitrage and frequency regulation in different market areas are maximized using Linrear Programming. A real-time optimal dispatch algorithm is proposed in [10] to maximize ESS's revenue from energy arbitrage in the day-ahead electricity market considering its contribution to transmission congestion relief. Financial benefits of BESSs in upgrade deferral of distribution networks were evaluated in [11]. Optimal operation of BESSs for mitigating PV variability and minimizing transformers' losses is studied in [12]. The optimal demand charge management for TOU customers using behind-the-meter energy storage is studied in [3, 13, 14].

Although the economic benefits of ESSs for different grid applications have been comprehensively investigated in the literature [2, 15, 16], most studies rely on the linear energy flow model that assumes energy storage efficiencies are constant. Using the linear models with constant storage efficiencies will cause suboptimal results because in practice ESSs' charge/discharge efficiencies vary as nonlinear functions of state-of-charge, temperature, charge/discharge power. However, the linear model is very commonly used in techno-economic studies due to the following reasons:

- The linear model can simplify the optimization problems to Linear Programming (LP) or Mixed Integer Linear Programming (MILP) problems which can be efficiently solved by any linear solvers. On the other hand, using nonlinear energy storage models introduces nonvexity into the optimization problems making them much harder to solve.
- The currently available technology-specific nonlinear models of energy storage only focus on the fast (miliseconds to seconds) dynamics of ESSs which are mostly used in control [17, 18] or in state estimation (e.g., state of charge estimation) [19–24]. However, these types of models are not suitable for the analyses that often examine long time periods (minutes to hours).

Therefore, in order to capture the technology-specific nonlinear characteristics in techno-economic analyses, it is essential to: 1) develop/derive the models that capture the ESSs' nonlinear behaviors over long periods of time; 2) develop analytical or numerical approaches that effectively solve the nonconvex optimization problems when incorporating these nonlinear models.

In this paper, we derive the nonlinear energy flow models for vanadium redox flow battery (VRFB), lead-acid, and li-ion battery systems. The models are incorporated into the

T. Nguyen, R. Byrne, and B. Chalamala, are with Sandia National Laboratories, Albuquerque, NM USA. e-mail: tunguy@sandia.gov. I. Gyuk is with the U.S. Department of Energy, Washington, DC USA.

TABLE I
ESS PARAMETERS

Symbol	Description
τ	Duration of one time period (e.g., one hour)
$\bar{P}$	Power rating of the inverter [MVA]
$\bar{S}$	Maximum energy capacity [MWh]
$\bar{Q}$	Maximum ampere-hour capacity [Ah]
$\bar{V}$	Rated DC Voltage [V]
S	State of charge [kWh]
T	Storage cell temperature [K]
γ_{s}	Calendar efficiency over one period [%]
γ_{c}	Energy storage charge efficiency [%]
γ_{d}	Energy storage discharge efficiency [%]
γ_{pcs}	Inverter efficiency [%]

optimization problem that maximizes the revenue of an ESS when participating in multiple activities in a market area. A Dynamic Programming approach is proposed to solve the nonconvex optimization. In this approach, the possible states of charge (SOC) at each time step are defined. A forward search algorithm is developed to find the optimum sequence of SOCs that generates the maximum revenue given the nonlinear charge/discharge power of the ESS. In order to improve the performance of the algorithm, parallel computation is used. To demonstrate the feasibility and effectiveness of the approach, a case study is conducted for maximzing the revenue of a Vanadium Redox Flow Battery system in PJMs energy and frequency regulation market.

II. ENERGY FLOW MODEL OF ENERGY STORAGE SYSTEMS

Energy flow models capture ESS's behaviors over long periods of time that often corresponds with the market time interval (e.g., hourly day ahead market for energy). The models provide insights into the charge/discharge profile, which is required in techno-economic analysis (e.g., feasibility study, long term planning, selection of the energy storage technology) [2].

Assuming the AC input power during charge $P_i^{\text{c}}(MW)$, the AC output power during discharge $P_i^{\text{d}}(MW)$ are nonnegative, the charge efficiency γ_{c} and discharge efficiency γ_{d} are constant, the state of charge (SOC) $S_i(MWh)$ at time i can be expressed as [25]:

$$S_i = \gamma_{\text{s}} S_{i-1} + \gamma_{\text{c}} P_i^{\text{c}} \tau - \frac{P_i^{\text{d}} \tau}{\gamma_{\text{d}}} \tag{1}$$

which states that the SOC at time i is the sum of the SOC at time $i-1$ and the net charging energy (adjusted with the storage charge/discharge efficiencies).

In practice, power losses during charge and discharge often vary as functions of SOC, temperature, and charge/discharge power [26]. Therefore, the SOC in (1) can be rewritten as:

$$S_i = \gamma_{\text{s}} S_{i-1} + \underbrace{f^{\text{c}}(P_i^{\text{c}}, S_{i-1}, T)}_{\text{Total charged power}} \tau - \underbrace{f^{\text{d}}(P_i^{\text{d}}, S_{i-1}, T)}_{\text{Total discharged power}} \tau \tag{2}$$

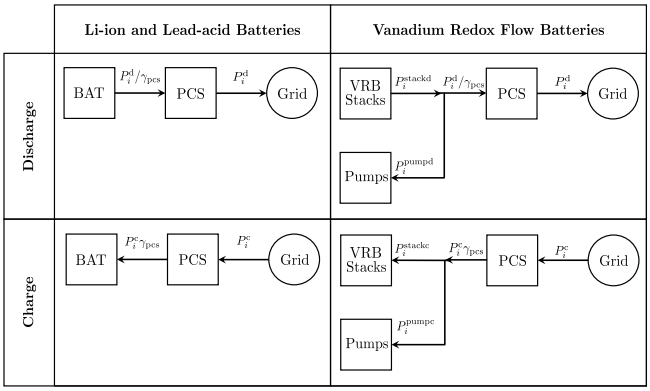

Fig. 1. The power flow of Batteries Energy Storage Systems (BESS)

Given that the temperature of a storage device is often maintained within an operating range by the thermal management system, we assume the temperature T is constant and equal to 25^oC in this paper. Therefore, the total charged power f^{c} and discharged power f^{d} are simplified as functions of charge/discharge power and the state of charge. The nonlinearity of these functions to the input/output power and the SOC are very dependent on the energy storage technologies. In this section, we characterized f^{c} and f^{d} of lead-acid, li-ion, and vanadium redox flow batteries (VRFB). The power flow of each battery energy storage system (BESS) is described in Figure 1. The storage parameters are shown in Table I.

A. Lead-acid and Li-ion battery

The power losses during charging or discharging lead-acid and li-ion batteries are mainly caused by the heat loss due to ohmic and polarization effects [27]. The power loss is approximately equal to the voltage drop (polarization) times the charge/discharge DC current:

$$P_{\text{loss}}(\text{W}) = \Delta V \times I \tag{3}$$

For lead-acid and lithium-ion batteries, the voltage drop is determined based on the empirical method presented in [21]:

- During discharge:

$$\Delta V^{\text{d}} = (R + \frac{K\bar{S}}{S}) I^{\text{d}} + \frac{K\bar{Q}(\bar{S} - S)}{S} \tag{4}$$

- During charge:

$$\Delta V^{\text{c}} = (R + \frac{K\bar{S}}{\bar{S} - S}) I^{\text{c}} + \frac{K\bar{Q}(\bar{S} - S)}{S} \tag{5}$$

where R and K are the model coefficients which can be calculated from manufacturer's data.

From (4), (5), the power losses (MW) during charge and discharge for lead acid and lithium-ion battery can be calculated as follows:

- During discharge:

$$\begin{aligned} P^{\text{ld}} &= 10^{-6}[(R + \frac{K\bar{S}}{S})(I^{\text{d}})^2 + \frac{K\bar{Q}(\bar{S} - S)}{S} I^{\text{d}}] \\ &\approx \frac{10^6}{\bar{V}^2}[(R + \frac{K\bar{S}}{S})(P^{\text{d}}/\gamma_{\text{pcs}})^2 + \frac{K\bar{S}(\bar{S} - S)}{S} P^{\text{d}}/\gamma_{\text{pcs}}] \end{aligned} \tag{6}$$

- During charge:

$$P^{\text{lc}} = 10^{-6}[(R + \frac{K\bar{S}}{\bar{S}-S})I^{\text{c}} + \frac{K\bar{Q}(\bar{S}-S)}{S}] \approx \frac{10^{6}}{\bar{V}^{2}}[(R + \frac{K\bar{S}}{\bar{S}-S})(\gamma_{\text{pcs}}P^{\text{c}})^{2} + \frac{K\bar{S}(\bar{S}-S)}{S}\gamma_{\text{pcs}}P^{\text{c}}] \tag{7}$$

As a result, the functions f^{c} and f^{d} can be derived as:

$$f^{\text{c}} = \gamma_{\text{pcs}}P^{\text{c}} - P^{\text{lc}} \tag{8}$$

$$f^{\text{d}} = P^{\text{d}}/\gamma_{\text{pcs}} + P^{\text{ld}} \tag{9}$$

B. Vanadium Redox Battery

The power loss of a vanadium redox battery during charge and discharge includes two components: power for pumping the electrolytes and stack loss power due to internal resistance and electrochemical process. The total charged power f^{c} and discharged power f^{d} can be calculated as follows:

- During discharge:

$$f^{\text{d}} = \frac{P^{\text{stackd}}}{\gamma^{\text{d}}} \tag{10}$$

where P^{stackd} is stack power during discharge that is the total of terminal power and the pump power; and γ^{d} is the efficiency that accounts for the internal power loss during discharge. Based on the empirical model proposed in [28], P^{stackd} and γ^{d} can be derived:

$$P^{\text{stackd}} = a_{\text{p}}^{\text{d}}P^{\text{d}}/\gamma_{\text{pcs}} + b_{\text{p}}^{\text{d}}S(S-\bar{S}) + c_{\text{p}}^{\text{d}} \tag{11}$$

$$\gamma^{\text{d}} = \frac{a_{\text{v}}^{\text{d}}P^{\text{d}}/\gamma_{\text{pcs}} + b_{\text{v}}^{\text{d}}S + c_{\text{v}}^{\text{d}}}{a_{\text{v}}^{\text{o}}S + b_{\text{v}}^{\text{o}}} \tag{12}$$

- During charge:

$$f^{\text{c}} = \gamma^{\text{c}}P^{\text{stackc}} \tag{13}$$

where P^{stackc} is stack power during charge that is the total power after subtracting the pump power; and γ^{c} is the efficiency that accounts for the internal power loss during charge. Based on the empirical model proposed in [28], P^{stackc} and γ^{c} can be derived:

$$P^{\text{stackc}} = (a_{\text{p}}^{\text{c}}S + b_{\text{p}}^{\text{c}})\gamma_{\text{pcs}}P^{\text{c}} + c_{\text{p}}^{\text{c}}S + d_{\text{p}}^{\text{c}} \tag{14}$$

$$\gamma^{\text{c}} = \frac{a_{\text{v}}^{\text{o}}S + b_{\text{v}}^{\text{o}}}{(a_{\text{v}}^{\text{c}}S + b_{\text{v}}^{\text{c}})\gamma_{\text{pcs}}P^{\text{c}} + c_{\text{v}}^{\text{c}}S + d_{\text{v}}^{\text{c}}} \tag{15}$$

The model coefficients in (11), (12), (14), and (15) can be specified using manufacturer's and testing data. In Table II, the coefficients are determined based on the testing data of a 5kW/20kWh VRB given in [28]. In practice VRB systems are often built by integrating a number of small standardized VRB modules. Therefore, we assume that the coefficients in Table II are representative of VRFB performance regardless of the system size.

TABLE II
VRB MODEL COEFFICIENTS

	a_y^{x}	b_y^{x}	c_y^{x}	d_y^{x}
(x,y) = (o,v)	$\frac{0.236}{\bar{S}}$	-0.9989	-	-
(x,y) = (d,v)	$\frac{-0.2833}{\bar{P}}$	$\frac{0.1325}{\bar{S}}$	0.9861	-
(x,y) = (d,p)	1.0334	$\frac{0.3454\bar{P}}{\bar{S}^2}$	$0.1192\bar{P}$	-
(x,y) = (c,v)	$\frac{0.1974}{\bar{P}\bar{S}}$	$\frac{0.1617}{\bar{P}}$	$\frac{0.1421}{\bar{S}}$	0.9748
(x,y) = (c,p)	$\frac{-0.128}{\bar{S}}$	1.05	$\frac{0.038\bar{P}}{\bar{S}}$	$-0.118\bar{P}$

TABLE III
NOMENCLATURES

Symbol	Description
N	The time horizon of the optimization
N_k	The number of intra-period time steps considered in activity k
$\mathbb{M}_e$	The set of energy related activities
$\mathbb{M}_p$	The set of power related activities
ρ_i^j	The price of energy related activity j at period i [$/MWh]
ρ_i^k	The price of power related activity k at period i [$/MW]
P_i^k	Decision variable: the power reserved for power related activity k at period i [MW]
$P_i^{\text{d}j}$, $P_i^{\text{c}j}$	Decision variables: the discharge and charge power allocated for energy related activity j at period i [MW]
$\sigma_{i,t}^{\text{d}k}$, $\sigma_{i,t}^{\text{c}k}$	The fraction of P_i^k that is actually called upon for discharging/charging at time step t of period i

III. OPTIMIZATION PROBLEM FORMULATION

In this paper the optimization is formulated to maximize the revenue of an ESS when participating in multiple activities in a market area. This includes the energy related activities like energy arbitrage and the power related activities like forward capacity and frequency regulation. The objective function is formulated as follows with the parameters and variables are defined in Table III:

$$\max \sum_{i=1}^{N}\left(\sum_{j\in\mathbb{M}_e}\rho_i^j(P_i^{\text{d}j} - P_i^{\text{c}j})\tau + \sum_{k\in\mathbb{M}_p}\rho_i^k P_i^k\right) \tag{16}$$

For example, for energy arbitrage and frequency regulation in PJM [29], the objective function can be written as:

$$\max \sum_{i=1}^{N}[\text{LMP}_i(P_i^{\text{d}} - P_i^{\text{c}})\tau + \tag{17}$$

$$(\beta_i^{\text{M}}\text{RMPCP}_i + \text{RMCCP}_i)\eta_i P_i^{\text{reg}}] \tag{18}$$

where LMP_i ($/MWh) is the local marginal price at time i; RMPCP_i ($/MW) and RMCCP_i ($/MW) are respectively the regulation performance clearing price and the regulation capacity clearing price at time i; β_i^{M} is the mileage ratio at time i; and η_i is the performance score at time i.

In practice, an ESS can participate in multiple market activities at one time period such as energy arbitrage together

with frequency regulation. However, stacking up activities at one time period might complicate the intra-period energy management of the ESS. Therefore, in this paper we assume the ESS is only allowed to participate in at most one market's activity at each time period i. The corresponding constraint is as follows:

$$\sum_{j\in\mathbb{M}_e}(\alpha_i^{\mathrm{d}j}+\alpha_i^{\mathrm{c}j})+\sum_{k\in\mathbb{M}_p}\alpha_i^k\leq 1\ \forall i \tag{19}$$

where α_i^x is a binary variable that activates activity x:

$$\alpha_i^x=\begin{cases}1 & \text{if } P_i^x\geq 0\\ 0 & \text{if } P_i^x=0\end{cases} \tag{20}$$

The condition in (20) can be represented by the following constraint:

$$0\leq P_i^x\leq \alpha_i^x\bar{P} \tag{21}$$

The other constraints for SOC management are also considered:

$$S_{\min}\leq S_i\leq S_{\max} \tag{22}$$

$$S_0=S_N \tag{23}$$

The state of charge S_i can be calculated based on (2):

$$\begin{aligned}S_i=&\gamma_{\mathrm{s}}S_{i-1}+\tau\sum_{j\in\mathbb{M}_e}[f^{\mathrm{c}}(P_i^{\mathrm{c}j},S_{i-1})-f^{\mathrm{d}}(P_i^{\mathrm{d}j},S_{i-1})]\\&+\tau\sum_{k\in\mathbb{M}_p}\frac{1}{N_k}\sum_{t=1}^{N_k}[f^{\mathrm{c}}(\sigma_{i,t}^{\mathrm{c}k}P_i^k,S_{i-1})-f^{\mathrm{d}}(\sigma_{i,t}^{\mathrm{d}k}P_i^k,S_{i-1})]\end{aligned} \tag{24}$$

For energy arbitrage and frequency regulation, S_i can be calculated as follows:

$$\begin{aligned}S_i=&\gamma_{\mathrm{s}}S_{i-1}+\tau[f^{\mathrm{c}}(P_i^{\mathrm{c}},S_{i-1})-f^{\mathrm{d}}(P_i^{\mathrm{d}},S_{i-1})]\\&+\underbrace{\frac{\tau}{N_r}\sum_{t=1}^{N_r}[f^{\mathrm{c}}(\sigma_{i,t}^{\mathrm{RD}}P_i^{reg},S_{i-1})-f^{\mathrm{d}}(\sigma_{i,t}^{\mathrm{RU}}P_i^{reg},S_{i-1})]}_{f_i^{\mathrm{reg}}(P_i^{\mathrm{reg}},S_{i-1})}\end{aligned} \tag{25}$$

where $\tau=1hr$ and N_r is the number of intra-hour time steps given for frequency regulation; $\sigma_{i,t}^{\mathrm{RD}}$ and $\sigma_{i,t}^{\mathrm{RU}}$ are the regulation up and regulation down signals given at time step t of hour i. For example, in PJM, the fast regulation signal (RegD) is sent to a regulation resource every 2 seconds; therefore, $N_r=1800$, $\sigma_{i,t}^{\mathrm{RU}}$ is the positive RegD, and $\sigma_{i,t}^{\mathrm{RD}}$ is absolute value of the negative RegD. It should be noted that while f^c and f_d are time-independent, f_i^{reg} is associated with each time period due to the temporal nature of the AGC signal.

IV. Dynamic Programming Approach

The above optimization has linear objective function. The ESS's constant-efficiency model in (1) is often used [9, 29, 30] with given maximum efficiencies and perfect-foresight data to estimate the maximum revenue of ESS in the best case scenario. The constant-efficiency model makes the constraints in (22) and (23) linear; therefore, the optimization problem can be formulated as a Linear Programming (LP) problem. However, this model ignores the underlying the dynamics of the energy storage device that makes the results less accurate.

The ESS's non-linear energy flow model in (2) can better capture the technology-specific characteristics of the energy storage devices; however, incorporating it into the optimization problem introduces the following challenges:

- Non-convexity: the constraints in (22) and (23) now become non-linear and non-convex that makes the optimization non-convex.
- Complex dynamics: the state of charge at time i is non-linear to both charge/discharge power and the state of charge at time $i-1$.

The above challenges make the problem become a sequential decision problem for which Dynamic Programming (DP) is well known. A DP-based method often finds the optimal path to the destination by breaking it down to a sequence of steps overtime. At each time step, the optimal subsequence to each feasible state can be found based on the optimal subsequences to the previous step. Finally, the optimal sequence can be found by repeating the above process until the time horizon is reached. The main advantage of DP is that it can find the global optimum by finding and memorizing the optimal subsequences.

In this paper, forward DP algorithm is applied. The algorithm is described in details in IV-A. Parallel computing, as described in IV-B, is used to improve the performance of the algorithm.

A. Forward DP algorithm

The algorithm is described in Fig. 3. The main procedures of the algorithm include:

1) Define the state space: The state space at each time step i, denoted as $\mathbb{S}_i$, is defined as follows:

$$\mathbb{S}_i=\{S_i\mid S_{min}\leq S_i\leq S_{max}\}\ \forall i<N \tag{26}$$

$$\mathbb{S}_N=\{S_N\} \tag{27}$$

with S_i is a possible state of charge of the ESS that satisfies constraints (22) and (23). This state space is an uncountably infinite set, which is not manageable by DP. Therefore, we discretize this state space by considering a finite number of the states that represent the space. For example, each element of $\mathbb{S}_i$ can represent an integer percentage of the state of charge:

$$\mathbb{S}_i=\left\{S_i^u=\frac{u}{100}\bar{S}\mid\ u\in\mathbb{N}\text{ and }S_{min}\leq S_i^u\leq S_{max}\right\} \tag{28}$$

2) Run forward to find the maximum revenue to each state: The maximum revenue if reaching state S_i^u at time i can be expressed as:

$$R(S_i^u)=\max_{S_{i-1}^v\in\mathbb{S}_{i-1}}\left\{R(S_{i-1}^v\rightarrow S_i^u)+R(S_{i-1}^v)\right\} \tag{29}$$

where $R(S_{i-1}^v)$ is the maximum revenue if going to state S_{i-1}^v, which is solved at the previous time period $i-1$. $R(S_{i-1}^v\rightarrow S_i^u)$ is the maximum revenue that can be generated

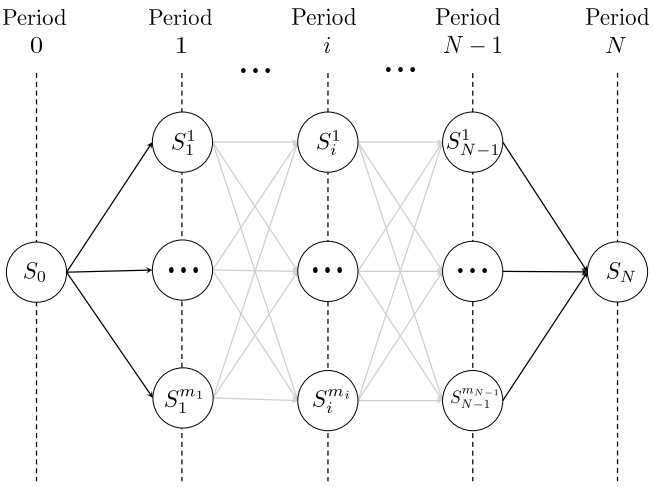

Fig. 2. State space of DP algorithm

by going from state S_{i-1}^v to state S_i^u; and it is the solution of the following optimization problem:

$$R(S_{i-1}^v \to S_i^u) = \max \left(\sum_{j\in\mathbb{M}_e} \rho_i^j (P_i^{\mathrm{d}j} - P_i^{\mathrm{c}j})\tau + \sum_{k\in\mathbb{M}_p} \rho_i^k P_i^k \right) \tag{30}$$

$s.t.$ (19), (21), and the following equality constraint:

$$\begin{aligned} S_i^u - \gamma_{\mathrm{s}} S_{i-1}^v = \tau \sum_{j\in\mathbb{M}_e} [f^{\mathrm{c}}(P_i^{\mathrm{c}j}, S_{i-1}^v) - f^{\mathrm{d}}(P_i^{\mathrm{d}j}, S_{i-1}^v)] + \\ \tau \sum_{k\in\mathbb{M}_p} \frac{1}{N_k} \sum_{t=1}^{N_k} [f^{\mathrm{c}}(\sigma_{i,t}^{\mathrm{c}k} P_i^k, S_{i-1}^v) - f^{\mathrm{d}}(\sigma_{i,t}^{\mathrm{d}k} P_i^k, S_{i-1}^v)] \end{aligned} \tag{31}$$

This is a nonconvex optimization because of the nonlinear equality constraint (31). This problem can be converted to a Mixed Integer Lear Programming (MILP) problem by piecewise linearizing $f^{\mathrm{c}}(P_i^{\mathrm{c}})$ and $f^d(P_i^{\mathrm{d}})$. The advantage of this method is that the global solution can always be found by an MIP solver. However, the piecewise linearization introduces a large amount of binaries and segment variables into the problem, which will significantly increase the computation burden of the overall dynamic programming algorithm. Therefore, we propose to numerically solve equation (31) for each market activity and then find the activity that generates the maximum revenue. The problem is reformulated as follows:

$$R(S_{i-1}^v \to S_i^u) = \max \left\{ \rho_i^{j^*} P_i^{\mathrm{d}j^*} \tau, -\rho_i^{j^\dagger} P_i^{\mathrm{c}j^\dagger} \tau, \rho_i^{k*} P_i^{k*} \right\} \tag{32}$$

in which

$$P_i^{\mathrm{d}j^*} = \underset{j\in\mathbb{M}_e}{\operatorname{argmax}} \left\{ \rho_i^j P_i^{\mathrm{d}j} | S_i^u - \gamma_{\mathrm{s}} S_{i-1}^v = -\tau f^{\mathrm{d}}(P_i^{\mathrm{d}j}, S_{i-1}^v) \right\} \tag{33}$$

$$P_i^{\mathrm{c}j^\dagger} = \underset{j\in\mathbb{M}_e}{\operatorname{argmax}} \left\{ -\rho_i^j P_i^{\mathrm{c}j} | S_i^u - \gamma_{\mathrm{s}} S_{i-1}^v = \tau f^{\mathrm{c}}(P_i^{\mathrm{c}j}, S_{i-1}^v) \right\} \tag{34}$$

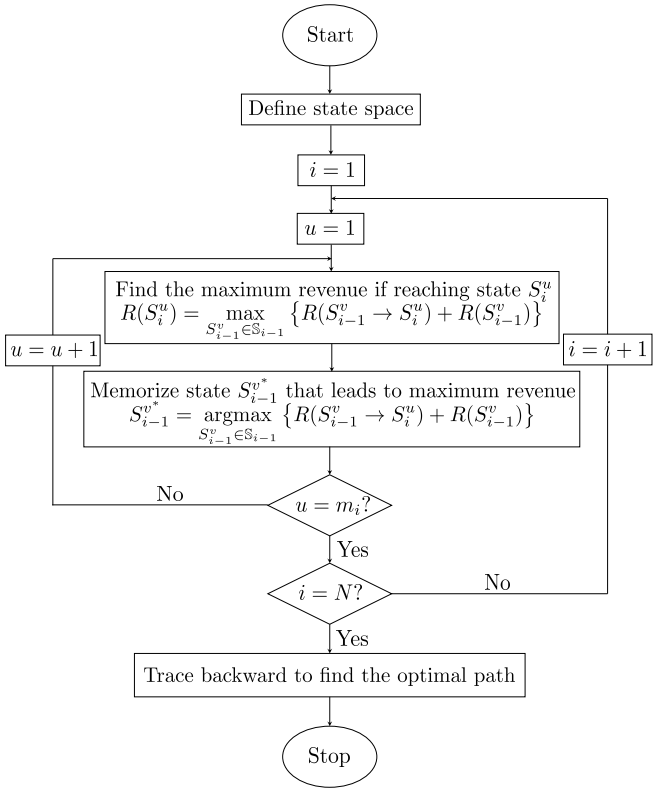

Fig. 3. Forward dynamic programming algorithm

$$\begin{aligned} P_i^{k*} = \underset{k\in\mathbb{M}_p}{\operatorname{argmax}} \Big\{ \rho_i^k P_i^k | S_i^u - \gamma_{\mathrm{s}} S_{i-1}^v = \frac{\tau}{N_k} \sum_{t=1}^{N_k} [f^{\mathrm{c}}(\sigma_{i,t}^{\mathrm{c}k} P_i^k, S_{i-1}^v) \\ - f^{\mathrm{d}}(\sigma_{i,t}^{\mathrm{d}k} P_i^k, S_{i-1}^v)] \Big\} \end{aligned} \tag{35}$$

Since S_{i-1}^v is known when solving (32), f^d and f^c are single-variable functions of the discharge and charge powers. Therefore, the equality constraints in (33), (34), and (35) can be solved using an iterative method. In this paper, we use Newton-Raphson iteration method which exhibits quadratic convergence.

3) Memorize optimal sub-paths and trace backward to find the optimal path: For each state S_i^u at time period i, the solutions of (29) and (32) are memorized:

$$D_i(S_i^u) = S_{i-1}^{v^*} = \underset{S_{i-1}^v \in \mathbb{S}_{i-1}}{\operatorname{argmax}} \left\{ R(S_{i-1}^v \to S_i^u) + R(S_{i-1}^v) \right\} \tag{36}$$

$$R(S_i^u) = R(S_{i-1}^{v^*} \to S_i^u) + R(S_{i-1}^{v^*}) \tag{37}$$

When the forward running process completes ($i = N$), backward tracing is performed to find the optimal path that creates the maximum revenue:

$$S_N^* = S_N,\ S_{i-1}^* = D_i(S_i^*),\ S_0^* = S_0 \tag{38}$$

B. The "curse of dimensionality" and parallel computation

Dynamic programming is a very powerful method to find the global optimum of a sequential decision problem. However,

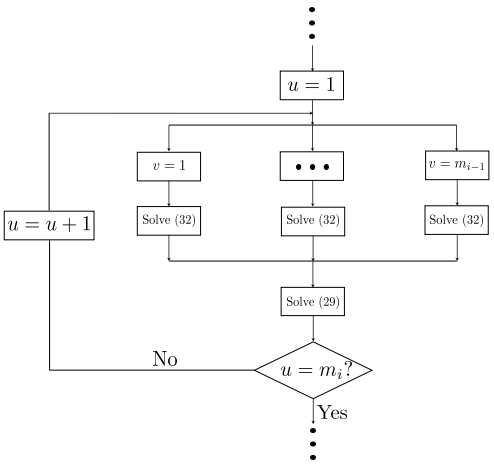

Fig. 4. Partial parallelization of the forward dynamic programming algorithm

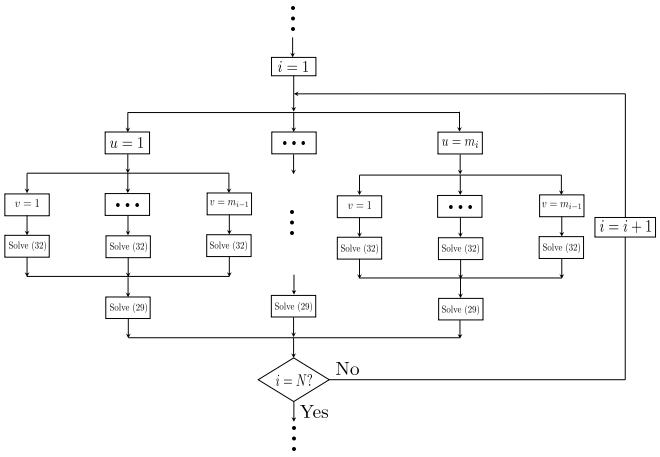

Fig. 5. Full parallelization of the forward dynamic programming algorithm

the method suffers from the notorious curse of dimensionality if the state space is high-dimensional. Asumming there are m_i feasible states at each time i and the time horizon is N, the total number of possible links between two consecutive periods is $\sum_{i=1}^{N} m_i m_{i-1}$. The computation time of the above forward dynamic programming algorithm can be estimated as follows:

$$T_\Sigma \approx \sum_{i=1}^{N} (T_{32} m_i m_{i-1} + T_{29} m_i) \tag{39}$$

where T_{32} and T_{29} are respectively the time for solving Eq. (32) and Eq. (29). It can be seen from (39) that if N and m_i are large the computation burden can be overwhelming. For example, if $m_i = 101$ (state of charge ={$0\%, ..., 100\%$}), $N = 744$ (744 hours of a 31-day month), and $T_{29} = T_{32} = 0.01sec$ then $T_\Sigma \approx 21hr$ which is very significant for an analysis of one month.

In order to reduce the computation time, we parallelize the computation of the forward running process. In theory, Eq. (32) can be solved in parallel for each link; similarly, Eq. (29) can be solved in parallel for each state after all the links are solved. Therefore, the theoretical computation time after a full parallelization (Fig. 4) is $T_\Sigma^{fp} \approx (T_{32} + T_{29})N$. However, due to the computers' physical limits, full parallelization might be impossible or ineffective in reducing computation time. In this work, we partially parallel the computation process (Fig. 4) by solving Eq. (32) in parallel for each link but solving Eq. (29) in series for each state. The theoretical computation time after a partial parallelization is $T_\Sigma^{pp} \approx \sum_{i=1}^{N} (T_{32} + T_{29}) m_i$.

V. A Case Study

In this section, we evaluate the maximum revenue of a Vanadium Redox Flow Battery (VRFB) System in PJM market area using nonlinear VRFB model and compare the results with the ones calculated using linear model. The market activities considered in this case study are day-ahead energy arbitrage and frequency regulation. The following inputs are considered:

- A VRFB system of $20MW/5MWh$ is considered: $\bar{S} = 5MWh$, $\bar{P} = 20MW$
- PJM historical price data from June 2016 to May 2017 are used.
- Hourly day-ahead LMP for node 51298 and Dynamic 2-second AGC signals (RegD signals) are used.
- The performance scores are assumed to be 1 at all time periods: $\eta_i = 1\ \forall i$.
- The mileage ratios β_i are calculated based on the historical regulation data.
- The efficiency of the PCS is approximated as: $\gamma_{\text{pcs}} = 0.95$.
- The integer-percentage SOCs are considered at each time period i: $\mathbb{S}_i = \{0\%\bar{S}, 1\%\bar{S}, ..., 100\%\bar{S}\}$
- The SOC is maintained at 50% at the beginning and the end of each month: $S_0 = S_N = 50\%\bar{S}$.
- The coefficients of the VRFB nonlinear model are calculated based on Table II.
- 70% round trip efficiency is used in the linear model.

The f^{d} (in Eq. (10)) , f^{c} (in Eq. (13)) and one example of f_i^{reg} (Eq. (in 25)) with i is the first hour of June are plotted in Fig. 6. The figures show the nonlinearity of f^{d}, f^{c}, and f_i^{reg} to the power output and the state of charge. It should be noted that, when then discharge power is close to zero, the VRFB is discharging some amount of power just to supply its own pumps. Similarly, when the charge power is small (less than about 5% of the rated power), the VRFB is also discharging a small amount of power consumed by its pumps. When doing energy arbitrage, these low-efficiency working regions can be avoided by reducing the pumps' speed to minimum if the charge/discharge power is low. However, when providing frequency regulation, the battery system has to follow a regulation signal as close as possible. This is because failing to comply the regulation signal could reduce the performance score and disqualify the system for the regulation market. In this case, variable speed control of the pumps is not effective in following the very fast regulation signal. Therefore, even though the output of the VRFB system can almost perfectly follow the regulation signals, its efficiency is low when the

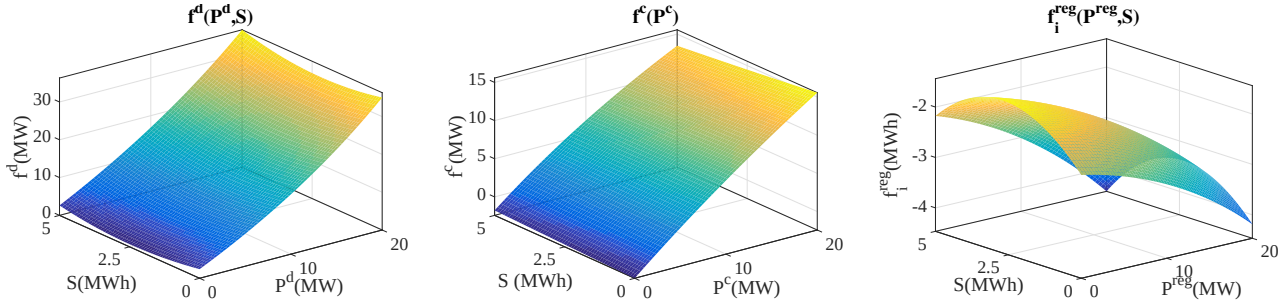

Fig. 6. f^{d}, f^{c}, and f_i^{reg} functions

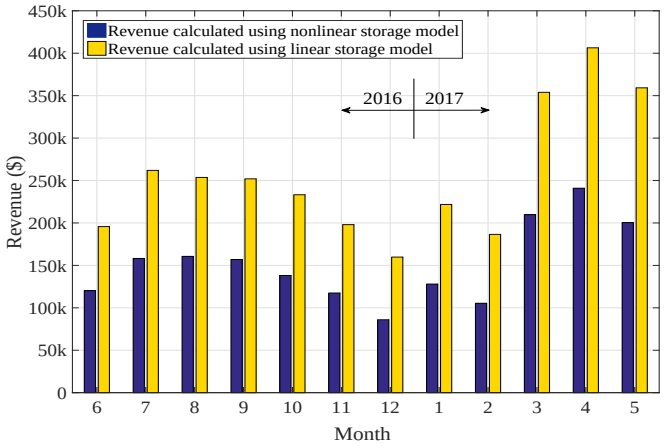

Fig. 7. 2016-2017 monthly revenue from arbitrage and frequency regulation.

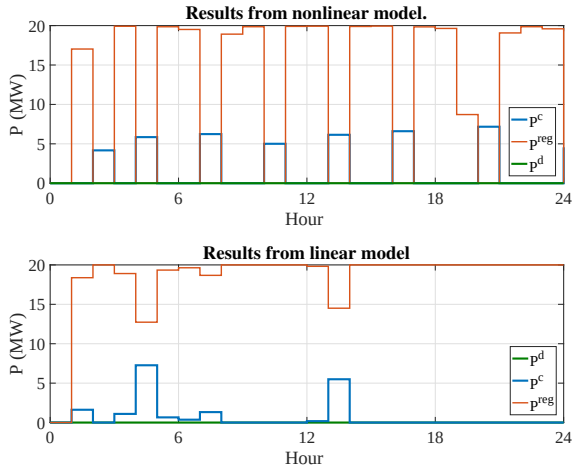

Fig. 8. Power output of the VRFB on the June 1st 2016

call-upon amount of regulation (in either direction) is low.

After calculating f^{d}, f^{c}, and f_i^{reg} functions, the dynamic programming algorithm is set up with 1-hour time period ($\tau = 1$) and 1-month time horizon. The maximum revenue for energy arbitrage and frequency regulation is solved for each month from June 2016 to May 2017. The monthly revenues calculated using nonlinear (so-called nonlinear revenues) and using linear storage models (so-called linear revenues) are shown in Fig. 7. The revenues from each market activity are given in Table IV for the nonlinear case and in Table V for the linear case. An example of 24-hr output powers of the VRFB calculated using nonlinear and linear models are plotted in Fig. 8. As seen in the results, the total nonlinear revenue is about one third lower than the linear one. The nonlinear regulation revenues are approximately 80% of the linear regulation revenues. On the other hand, the nonlinear arbitrage revenues are much more negative than the linear ones, which means more charging is required to balance the state of charge. This is because the nonlinear model captures more precisely the low-efficiency working operations when following regulation signals.

The computation for this analysis is performed by an Intel Xeon CPU E5-2687 (4-core) processor. The average time for an 1-month analysis by the DP algorithm is approximately 2.25hr if partial paralellization is used. This shows the feasibility of the proposed DP-based approach in dealing with the non-linear storage model.

VI. Conclusions

In this paper, the nonlinear energy flow models for vanadium redox flow battery (VRFB), lead-acid, and li-ion battery systems have been derived. Incorporating the nonlinear storage models introduces more complex dynamics and nonconvexity into the optimization problem. A DP-based approach is proposed to solve the nonconvex optimization, in which a forward search algorithm is developed to find the optimum sequence of SOCs that generates the maximum revenue given the nonlinear charge/discharge power of the ESS. A case study is conducted for maximzing the revenue of a Vanadium Redox Flow Battery system in PJMs energy and frequency regulation market. The results show the nonlinear models can capture more precisely the low-efficiency working regions of the VRFB thereby improving the accuracy of the calculated revenues. The proposed DP-based algorithm has also shown its feasibility in solving the nonconvex optimization problems.

VII. Acknowledgment

Sandia National Laboratories is a multi-mission laboratory managed and operated by National Technology and Engineering Solutions of Sandia, LLC., a wholly owned subsidiary of Honeywell International, Inc., for the U.S. Department of Energy National Nuclear Security Administration under contract DE-NA-0003525. The authors would like to thank DOE Office of Electricity Delivery and Energy Reliability, Energy Storage Research program for funding this research.

TABLE IV
ARBITRAGE AND REGULATION REVENUES (USING NONLINEAR MODEL)

Month	Regulation ($)	Arbitrage ($)	Total ($)
$2016-6$	$174,263$	$-29,996$	$144,268$
$2016-7$	$225,020$	$-35,180$	$189,840$
$2016-8$	$224,442$	$-31,672$	$192,770$
$2016-9$	$226,713$	$-38,404$	$188,309$
$2016-10$	$209,263$	$-43,552$	$165,711$
$2016-11$	$175,695$	$-34,715$	$140,980$
$2016-12$	$138,373$	$-35,224$	$103,148$
$2017-1$	$179,565$	$-25,957$	$153,608$
$2017-2$	$146,097$	$-19,621$	$126,476$
$2017-3$	$275,352$	$-23,654$	$251,698$
$2017-4$	$318,409$	$-29,277$	$289,132$
$2017-5$	$273,902$	$-33,510$	$240,393$
Total	$2,567,095$	$-380,761$	$2,186,333$

TABLE V
ARBITRAGE AND REGULATION REVENUES (USING LINEAR MODEL)

Month	Regulation ($)	Arbitrage ($)	Total ($)
$2016-6$	$200,834$	$-5,118$	$195,715$
$2016-7$	$267,493$	$-5,532$	$261,961$
$2016-8$	$257,765$	$-4,099$	$253,666$
$2016-9$	$260,900$	$-8,919$	$251,981$
$2016-10$	$244,238$	$-11,010$	$233,228$
$2016-11$	$206,793$	$-8,801$	$197,992$
$2016-12$	$170,349$	$-10,559$	$159,790$
$2017-1$	$229,958$	$-8,117$	$221,842$
$2017-2$	$196,703$	$-10,157$	$186,546$
$2017-3$	$361,181$	$-7,229$	$353,952$
$2017-4$	$422,557$	$-16,192$	$406,365$
$2017-5$	$381,241$	$-22,023$	$359,218$
Total	$3,200,014$	$-117,756$	$3,082,258$

REFERENCES

[1] D. Manz, R. Walling, N. Miller, B. LaRose, R. D'Aquila, and B. Daryanian, "The grid of the future: Ten trends that will shape the grid over the next decade," *IEEE Power and Energy Magazine*, vol. 12, no. 3, pp. 26–36, May 2014.

[2] R. H. Byrne, T. A. Nguyen, D. A. Copp, B. R. Chalamala, and I. Gyuk, "Energy management and optimization methods for grid energy storage systems," *IEEE Access*, vol. PP, no. 99, pp. 1–1, 2017.

[3] T. Nguyen and R. Byrne, "Maximizing the cost-savings for time-of-use and net-metering customers using behind-the-meter energy storage systems," in *Proceedings of the 2017 North American Power Symposium (NAPS)*, Morgantown, WV, Sept 2017, pp. 1–5.

[4] (2011) Analytic challenges to valuing energy storage. [Online]. Available: https://www1.eere.energy.gov/analysis/pdfs/analytic_challenges_to_valuing_energy_storage_workshop_report.pdf

[5] Y. J. Zhang, C. Zhao, W. Tang, and S. H. Low, "Profit maximizing planning and control of battery energy storage systems for primary frequency control," *IEEE Transactions on Smart Grid*, vol. PP, no. 99, pp. 1–1, 2016.

[6] R. H. Byrne and C. A. Silva-Monroy, "Estimating the maximum potential revenue for grid connected electricity storage: Arbitrage and the regulation market," Sandia National Laboratories, Albuquerque, NM, SAND2012-3863, resreport, 2012.

[7] ——, "Potential revenue from electrical energy storage in ercot: The impact of location and recent trends," in *2015 IEEE Power Energy Society General Meeting*, July 2015, pp. 1–5.

[8] R. H. Byrne, R. J. Conception, and C. A. Silva-Monroy, "Estimating potential revenue from electrical energy storage in pjm," in *2016 IEEE Power Energy Society General Meeting*, July 2016, pp. 1–5.

[9] T. Nguyen, R. Byrne, R. Conception, and I. Gyuk, "Maximizing revenue from electrical energy storage in MISO energy & frequency regulation markets," in *Proceedings of the 2017 IEEE Power Energy Society General Meeting*, Chicago, IL, July 2017, pp. 1–5.

[10] H. Khani, M. R. D. Zadeh, and A. H. Hajimiragha, "Transmission congestion relief using privately owned large-scale energy storage systems in a competitive electricity market," *IEEE Transactions on Power Systems*, vol. 31, no. 2, pp. 1449–1458, March 2016.

[11] S. R. Deeba, R. Sharma, T. K. Saha, D. Chakraborty, and A. Thomas, "Evaluation of technical and financial benefits of battery-based energy storage systems in distribution networks," *IET Renewable Power Generation*, vol. 10, no. 8, pp. 1149–1160, 2016.

[12] A. Nagarajan and R. Ayyanar, "Design and strategy for the deployment of energy storage systems in a distribution feeder with penetration of renewable resources," *IEEE Transactions on Sustainable Energy*, vol. 6, no. 3, pp. 1085–1092, July 2015.

[13] J. Neubauer and M. Simpson, "Deployment of behind-the-meter energy storage for demand charge reduction," 2015.

[14] D. Wu, M. Kintner-Meyer, T. Yang, and P. Balducci, "Economic analysis and optimal sizing for behind-the-meter battery storage," in *2016 IEEE Power and Energy Society General Meeting (PESGM)*, July 2016, pp. 1–5.

[15] J. Eyer and G. Corey, "Energy storage for the electricity grid: Benefits and market potential assessment guide," Sandia National Laboratories, Albuquerque, NM, SAND2010-0815, Tech. Rep., Feb 2010.

[16] A. Castillo and D. F. Gayme, "Grid-scale energy storage applications in renewable energy integration: A survey," *Energy Conversion and Management*, vol. 87, no. Supplement C, pp. 885 – 894, 2014. [Online]. Available: http://www.sciencedirect.com/science/article/pii/S0196890414007018

[17] P. Golchoubian and N. L. Azad, "Real-time nonlinear model predictive control of a battery 8211;supercapacitor hybrid energy storage system in electric vehicles," *IEEE Transactions on Vehicular Technology*, vol. 66, no. 11, pp. 9678–9688, Nov 2017.

[18] H. E. Fadil, F. Giri, J. M. Guerrero, and A. Tahri, "Modeling and nonlinear control of a fuel cell/supercapacitor hybrid energy storage system for electric vehicles," *IEEE Transactions on Vehicular Technology*, vol. 63, no. 7, pp. 3011–3018, Sept 2014.

[19] A. Szumanowski and Y. Chang, "Battery management system based on battery nonlinear dynamics modeling," *IEEE Transactions on Vehicular Technology*, vol. 57, no. 3, pp. 1425–1432, May 2008.

[20] I. S. Kim, "Nonlinear state of charge estimator for hybrid electric vehicle battery," *IEEE Transactions on Power Electronics*, vol. 23, no. 4, pp. 2027–2034, July 2008.

[21] O. Tremblay and L.-A. Dessaint, "Experimental validation of a battery dynamic model for ev applications," *World Electric Vehicle Journal*, vol. 3, no. 1, pp. 1–10, 2009.

[22] H. He, R. Xiong, and J. Fan, "Evaluation of lithium-ion battery equivalent circuit models for state of charge estimation by an experimental approach," *Energies*, vol. 4, no. 4, pp. 582–598, 2011.

[23] Y. Ma, B. Li, G. Li, J. Zhang, and H. Chen, "A nonlinear observer approach of soc estimation based on hysteresis model for lithium-ion battery," *IEEE/CAA Journal of Automatica Sinica*, vol. 4, no. 2, pp. 195–204, April 2017.

[24] B. Wang, Z. Liu, S. E. Li, S. J. Moura, and H. Peng, "State-of-charge estimation for lithium-ion batteries based on a nonlinear fractional model," *IEEE Transactions on Control Systems Technology*, vol. 25, no. 1, pp. 3–11, Jan 2017.

[25] P. Mokrian and M. Stephen, "A stochastic programming framework for the valuation of electricity storage," in *26th USAEE/IAEE North American Conference*, 2006, pp. 24–27.

[26] T. A. Nguyen and M. L. Crow, "Stochastic optimization of renewable-based microgrid operation incorporating battery operating cost," *IEEE Transactions on Power Systems*, vol. 31, no. 3, pp. 2289–2296, 2016.

[27] H. A. Kiehne, *Battery technology handbook*. CRC Press, 2003, vol. 60.

[28] T. A. Nguyen, X. Qiu, J. D. Guggenberger II, M. L. Crow, and A. C. Elmore, "Performance characterization for photovoltaic-vanadium redox battery microgrid systems," *IEEE Transactions on Sustainable Energy*, vol. 5, no. 4, pp. 1379–1388, 2014.

[29] R. H. Byrne, R. Concepcion, and C. A. Silva-Monroy, "Potential revenue from electrical energy storage in PJM," in *Proceedings of the 2016 IEEE Power and Energy Society (PES) General Meeting*, Boston, MA, July 2016, pp. 1–5.

[30] R. H. Byrne and C. A. Silva-Monroy, "Potential revenue from electrical energy storage in ERCOT: The impact of location and recent trends," in *Proceedings of the 2015 IEEE Power and Energy Society (PES) General Meeting*, Denver, CO, July 2015, pp. 1–5.